INSTITUTE OF PHYSICS PUBLISHING SEMICONDUCTOR SCIENCE AND TECHNOLOGY

Semicond. Sci. Technol. **21** (2006) 1244–1249 doi:10.1088/0268-1242/21/9/006

On the thermal stability of high-voltage rectifier diodes

T T Mnatsakanov[1], M E Levinshtein[2], A S Freidlin[1] and J W Palmour[3]

[1] All-Russia Electrotechnical Institute, Krasnokazarmennaya 12, 111250 Moscow, Russia
[2] The Ioffe Physico-Technical Institute, Politekhnicheskaya 26, 194021 St Petersburg, Russia
[3] Cree Inc., 4600 Silicon Drive, Durham, NC 27703, USA

Received 4 April 2006, in final form 22 June 2006
Published 21 July 2006
Online at stacks.iop.org/SST/21/1244

Abstract
An analytical theory that makes it possible to determine the parameters of inversion points in current–voltage characteristics of high-voltage p–i–n rectifier diodes is suggested. All the main nonlinear processes (electron–hole scattering (EHS), Auger recombination, gap narrowing in a highly doped emitter) are considered. The temperature dependences of all the main parameters, including the bandgap, carrier (electron and hole) mobilities and diffusion coefficients, EHS, contact resistance and nonequilibrium carrier lifetime are taken into account. The predictions of the theory are compared with the results of adequate numerical experiments for a high-voltage (10 kV class) 4H-SiC p^+–i–n diode. The numerical data obtained coincide well with the predictions of the analytical theory.

1. Introduction

The ability to withstand current surges is one of the most important requirements for p–i–n rectifier diodes. Such surge currents appear rather frequently due to short circuits or high-power electromagnetic discharges. From the physical point of view, one of the most important criteria that can be used to assess the ability of a diode to withstand current surges is the type of the temperature dependence of its current–voltage (I–V) characteristic.

If the isothermal (pulsed) voltage drop *increases* with temperature at a given current (figure 1(*a*)), the self-heating of the device leads to a decrease in the current at a given bias. In this case, the diode is relatively thermally stable. If, by contrast, the isothermal voltage drop at a given current *decreases* as the temperature becomes higher (figure 1(*b*)), the current increases due to self-heating at a given bias. Such a situation can easily lead to thermal instability. Indeed, as can be seen in figure 1(*b*), a negative differential resistance inevitably appears in this case if the current density j is high enough. When the diode operates under voltage control, a current jump accompanied by a strong increase in the current density, filamentation, overheating and degradation may occur.

At small current densities, the isothermal voltage drop across the p–i–n structure *always decreases* as the temperature increases at a given current, because the main contribution to the forward drop comes in this case from the drop across the p–n junction, V_{pn}. The value of V_{pn} decreases as the temperature becomes higher due to a sharp increase in the intrinsic carrier concentration n_i (see, for example, [1, 2]). However, the isothermal forward voltage drop may, by contrast, *increase* with temperature at higher current densities (so-called inversion).

In Si p–i–n diodes, the inversion point commonly corresponds to current densities of about several tens of amperes per square centimetre. Hence, the temperature dependence of the I–V characteristic corresponds to the case shown in figure 1(*a*) not only in the case of current surges, but even at the ordinary operating current densities.

In high-voltage SiC p–i–n diodes, the inversion was observed in [3, 4]. In diodes with a blocking voltage of 6 kV, the inversion point corresponded to very high values of j of about 2500 A cm^{-2} [3]. At the same time, in SiC diodes with a 20 kV blocking voltage, two inversion points have been observed [4]. At small $j \leqslant 1$ A cm^{-2}, the temperature coefficient of the voltage drop was, as usually, negative. At intermediate values of j, 1 A cm^{-2} $\leqslant j \leqslant$ 50 A cm^{-2}, the conventional inversion effect was observed. However at higher current densities $j \geqslant 100$ A cm^{-2}, the second inversion point was observed at $T \sim 500$ K: the forward voltage drop again decreased as the temperature became higher.

Computer calculations of current–voltage characteristics of high-voltage p–i–n diodes have been extensively reported, especially for Si rectifier diodes. However, to the best of

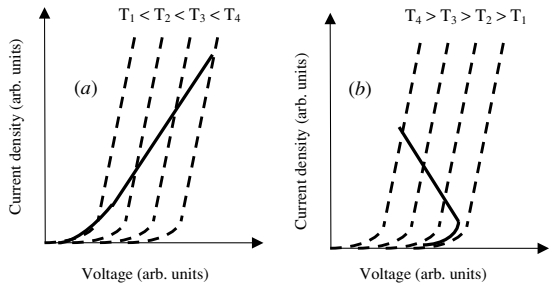

Figure 1. Qualitative current–voltage characteristics of forward-biased p–n junctions. The dashed lines show isothermal (pulsed) characteristics: (*a*) forward voltage drop *increases* with temperature ($T_1 < T_2 < T_3 < T_4$); (*b*) forward voltage drop *decreases* as the temperature increases ($T_1 < T_2 < T_3 < T_4$). Solid lines show the corresponding qualitative dc characteristics: the temperature of the diode increases with the current owing to self-heating.

our knowledge, there has been no analytical approach to the inversion point problem until now. Meantime, only an analytical theory allows one to judge the reliability of numerical calculations and to avoid the inevitable 'enumeration of possibilities' in computer experiments and simulations.

In this paper, an analytical theory that makes it possible to determine the parameters of the inversion points in high-voltage p–i–n diodes is suggested. Numerical estimates are obtained for 10 kV 4H-SiC diodes. The results obtained are compared with an adequate computer simulation.

2. The statement of the problem

The main idea of an analytical study of the inversion points consists in calculating the derivative $\frac{dV}{dT}$ and then solving the equation $\frac{dV}{dT} = 0$. The total voltage drop across the p^+–i–n^+ structure is determined by the well-known expression (see, for example [3])

$$V = V_{pn} + V_{TL} + V_{Teh} + V_C + V_S, \tag{1}$$

where $V_{pn} = \frac{kT}{q} \ln\left(\frac{p(0)p(W)}{n_{i0}^2}\right)$ is the voltage drop across the emitter–base junctions; q is the elementary charge; k is the Boltzmann constant; T is the temperature; n_{i0} is the intrinsic carrier concentration and $p(0)$ and $p(W)$ are the boundary carrier concentrations at the p^+–n and n^+–n junctions, respectively (for definiteness, we consider here the p^+–n–n^+ structure).

$$V_{TL} = \frac{\pi}{2}\left(\frac{jL}{q(\mu_n + \mu_p)}\right)\frac{\exp(W/2L)}{\sqrt{p(0)p(W)}}$$

is the voltage drop across the base n-layer due to all the scattering mechanisms except EHS, i.e., scattering on phonons, impurities, dislocations, etc. Here, $L = \sqrt{\frac{2b}{b+1}D_p\tau} = \sqrt{D\tau}$ is the ambipolar diffusion length; $b = \mu_n/\mu_p$, where μ_n and μ_p are electron and hole mobilities, respectively; D_p is the hole diffusion coefficient; τ is the lifetime of minority carriers (holes) at a high injection level and W is the width of the blocking n-base.

$V_{Teh} = \frac{jW}{qGp_0}$ is the EHS-related ohmic voltage drop across the base n-layer. Here G and p_0 are constants characterizing the EHS in a semiconductor [5]. The EHS-related component of the carrier mobility, μ_{np}, is described by the convenient expression $\mu_{np} = Gp_0/p$ [5].

$V_C = jR_C$ is the contact voltage drop, where R_C is the total contact resistance.

$V_S = \frac{jW_n^+}{qN_D^+\mu_n^+} \equiv jR_S$ is the voltage drop across the substrate, where R_S is the substrate resistance, and W_n^+, N_D^+, μ_n^+ are the width, doping level and electron mobility in the n^+ substrate respectively.

All the five components of the total voltage drop are temperature dependent. Let us consider the character of these temperature dependences.

The temperature dependences of $p(0)$ and $p(W)$ can be written (see, for example, [6]) as

$$p(0) = n_{i0}\sqrt{\frac{b}{b+1}\left(\frac{j}{j_{sn}}\right)},$$
$$p(W) = n_{i0}\sqrt{\frac{1}{b+1}\left(\frac{j}{j_{sp}}\right)}, \tag{2}$$

where j_{sn} and j_{sp} are the saturation currents of the p^+–n and n^+–n junctions, respectively. Taking into account the bandgap narrowing at a high doping level, Auger recombination and EHS in the emitters, the expression for the effective saturation current j_s can be written as [7]

$$\frac{j_s}{n_{i0}^2} = \frac{\sqrt{j_{sn}j_{sp}}}{n_{i0}^2} = q\sqrt[4]{C_n^+\tilde{D}_n^+C_p^+\tilde{D}_p^+}\exp\left(\frac{\Delta E_g}{kT}\right) \tag{3}$$

where

$$\tilde{D}_n^+ = D_n^+\frac{\mu_{np}}{\mu_{np}+\mu_n^+}, \qquad \tilde{D}_p^+ = D_p^+\frac{\mu_{pn}}{\mu_{pn}+\mu_p^+},$$

or

$$\left(\frac{j_s}{n_{io}^2}\right)(T) = \left(\frac{j_s}{n_{io}^2}\right)(T_0) \times \left(\frac{T}{T_0}\right)^{\delta}\exp\left[\frac{\Delta E_g}{kT_0}\left(\frac{T_0}{T}-1\right)\right]. \tag{4}$$

Here $T_0 = 300$ K; C_n^+,C_p^+, $D_n^+D_p^+$ are the Auger coefficients and diffusion coefficients in highly doped p^+ and n^+ layers, respectively; $\mu_{np} = Gp_0/N_A^+$ and $\mu_{pn} = Gp_0/N_D^+$ are mobilities in the p^+- and n^+-emitters, associated with EHS and ΔE_g is the bandgap narrowing.

The values of C_n^+,C_p^+, $D_n^+D_p^+$, ΔE_g and their temperature dependences in Si are known quite well (see, for example, [8]). In SiC, the values of Auger recombination have been measured only at room temperature [9]. Therefore, the temperature dependences of C_n^+ and C_p^+ in SiC were taken to be similar to the corresponding dependences in Si [10]. The temperature dependences of D_n^+,D_p^+ and the doping dependence of ΔE_g were inferred from the data of [9]. The estimate of δ in equation (4) gives $\delta \approx 1.6$ with account of the Auger recombination, EHS and bandgap narrowing.

The temperature dependence of the bandgap $E_g(T)$ was approximated by the Varshni equation [11]

$$E_g(T) = E_g(0) - a\frac{T^2}{T+T_1}\ \text{(eV)}. \tag{5}$$

For Si $a = 4.73 \times 10^{-4}$ eV, $T_1 = 636$ K; for SiC $a = 6.5 \times 10^{-4}$ eV, $T_1 = 1300$ K [8, 9].

The temperature dependences of the electron and hole mobilities μ_n and μ_p for $T > T_0$ can be approximated by

$$\mu_n(T) = \mu_n(T_0)\left(\frac{T}{T_0}\right)^{-\lambda} \quad \text{and}$$
$$\mu_p(T) = \mu_p(T_0)\left(\frac{T}{T_0}\right)^{-\lambda}. \tag{6}$$

For Si $\lambda = 2.2$ [8]; for SiC $\lambda = 2.6$ [9].

The temperature dependences of the diffusion length L differ substantially in Si and SiC. The hole lifetime τ in Si increases rather weakly with temperature; the increase in lifetime is virtually compensated by a decrease in the diffusion coefficient D, so that the W/L ratio in Si diodes can be considered to be temperature independent.

The lifetime in SiC (both p- and n-type) exponentially depends on temperature [12, 13]:

$$\tau(T) = \tau(T_0)\exp\left[\frac{\Delta}{kT_0}\left(1 - \frac{T_0}{T}\right)\right], \tag{7}$$

where $\Delta = 0.11$ eV.

In this case, the temperature dependence of L is given by

$$L(T) = L(T_0)\left(\frac{T}{T_0}\right)^{-\frac{\lambda-1}{2}}\exp\left[\frac{\Delta}{2kT_0}\left(1 - \frac{T_0}{T}\right)\right]. \tag{8}$$

In view of the fact that the EHS is caused by the Coulomb interaction, the temperature dependence of the constant Gp_0 was taken to be

$$(Gp_0)(T) = (Gp_0)(T_0)\left(\frac{T}{T_0}\right)^{\alpha}, \tag{9}$$

where $\alpha = 1.5$.

For temperature dependence of the contact resistance $R_C(T)$, a simple power dependence was used:

$$R_C(T) = R_C(T_0)\left(\frac{T}{T_0}\right)^{\beta}. \tag{10}$$

Depending on the type of the contacts and on specific features of the fabrication process, the value of β may widely vary. Moreover, β may be negative or positive, depending on the type of the contacts. For contacts to silicon carbide both negative and positive values of β have been observed.

To take into account the temperature dependence of the substrate resistance, the standard expression $R_S = \left[qN_d^+\mu_n\left(N_d^+, T\right)\right]^{-1}$ was used (N_d^+ is the concentration of ionized donors in the substrate). The temperature and concentration dependences of the mobility $\mu_n\left(N_d^+, T\right)$ were calculated according to [8]. The $R_S(T)$ dependence can be written in the form

$$R_S(T) = R_S(T_0)\left(\frac{T}{T_0}\right)^{\gamma}. \tag{11}$$

The following values were used in this paper: $\Delta E_g = 0.15$ eV and $\gamma = 0.15$ (which correspond to the case of a homogeneous doping level of the emitter equal to 5×10^{19} cm^{-3}), $\beta = 2.25$ [3], $Gp_0 = 5.8 \times 10^{19}$ V^{-1} cm^{-1} s^{-1} [3].

3. Results and discussion

Carrying out simple, but cumbersome calculations, we can obtain from (2)–(11) the following expressions for the derivatives of the terms in equation (1):

$$\frac{dV_{pn}}{dT} = \frac{1}{T}\left[V_{pn} - \frac{(E_g - \Delta E_g)}{q}\right], \tag{12}$$
$$\frac{dV_{TL}}{dT} = \frac{V_{TL}}{T}\varphi(T), \tag{13}$$

where

$$\varphi(T) = \frac{\lambda + 1 + \delta}{2} - \frac{\Delta E_g - \Delta}{2kT} - \left(\frac{W}{2L(T)}\right)\left[\frac{\Delta}{2kT} - \frac{\lambda - 1}{2}\right], \tag{14}$$
$$\frac{dV_{Teh}}{dT} = -\alpha\frac{V_{Teh}}{T}, \tag{15}$$
$$\frac{dV_C}{dT} = \beta\frac{V_C}{T}, \tag{16}$$
$$\frac{dV_S}{dT} = \gamma\frac{V_S}{T}. \tag{17}$$

Then the condition $\frac{dV}{dT} = 0$ takes the form

$$\left[V_{pn}(T) - \frac{(E_g(T) - \Delta E_g)}{q}\right] + V_{TL}\varphi(T) + (-\alpha V_{Teh}(T) + \beta V_C(T) + \gamma V_S(T)) = 0. \tag{18}$$

It is noteworthy that the terms V_{Teh}, V_C and V_S are directly proportional to the current density j: $V_{Teh} = \frac{jW}{qGp_0} \equiv R_{eh}j$, $V_C = R_C(T)j$, $V_S = \frac{jW_n^+}{qN_D^+\mu_n^+} \equiv R_S(T)j$. The term V_{TL} is proportional to $j^{1/2}$: $V_{TL}(T) = B_1(T)\sqrt{j}$, where

$$B_1(T) = \frac{\pi}{2}\left(\frac{L}{q(\mu_n + \mu_p)}\right)\frac{\exp(W/2L)}{\sqrt{\left(\frac{p(0)p(W)}{j}\right)}}. \tag{19}$$

Then, neglecting the logarithmically weak dependence of V_{pn} on j, we can derive from (18) the quadratic equation in $x \equiv \sqrt{j}$:

$$A(T) + B(T)x + C(T)x^2 = 0, \tag{20}$$

where

$$A(T) = \left[V_{pn}(T) - \frac{(E_g(T) - \Delta E_g)}{q}\right],$$
$$B(T) = B_1(T)\varphi(T),$$
$$C(T) = (-\alpha R_{eh}(T) + \beta R_C(T) + \gamma R_S(T)).$$

The roots of equation (20) determine the possible points of intersection of the current–voltage characteristics, i.e., the inversion points. Analysing equation (20), we can make some general conclusions concerning the inversion points in p–i–n diodes.

Let us note first that the term $A(T)$ in (20) is always negative ($A(T) < 0$), which corresponds to the well-known fact mentioned above: at small current densities ($j \to 0$), the derivative $\frac{dV}{dT}$ is negative $\left(\frac{dV}{dT} < 0\right)$, i.e., the isothermal forward voltage drop *decreases* as the temperature becomes higher.

The $B(T)$ and $C(T)$ dependences are determined by contributions of different effects. The contribution to $B(T)$ comes from the temperature dependences of the electron and

hole mobilities (see equation (6)), hole lifetime (see (7) and (8)), bandgap narrowing and Auger recombination in highly doped layers (see equations (3) and (4)). The main contribution to $C(T)$ comes from the temperature dependences of EHS, contact resistance and substrate resistance (equations (9)–(11)). Depending on the parameters of a p–i–n structure, $B(T)$ and $C(T)$ may be positive or negative.

The coefficients in equation (20) are temperature dependent. This means that the roots of equation (20), j_{in}, are also functions of temperature T. Hence, the isothermal I–V characteristics at, for example, $T = 300$ K and $T = 320$ K can intersect at some current density $j_{in} = j_1$, whereas isothermal I–V characteristics at, say, $T = 500$ K and $T = 520$ K intersect at another current density $j_{in} = j_2$ (or do not intersect at all), and so on.

Equation (20) can have two positive roots corresponding to two inversion points, just one positive root corresponding to a single inversion point, and no roots, which corresponds to the absence of an inversion point.

Two inversions points take place (at $A(T) < 0$) if

$$B(T) > 0, \qquad C(T) < 0. \tag{21}$$

Taking into account that $B(T) = B_1(T)\varphi(T)$, and $B_1(T) > 0$, we can easily find that the condition for existence of two inversion points can be written as

$$\varphi(T) = \frac{\lambda + 1 + \delta}{2} - \frac{\Delta E_g - \Delta}{2kT} - \left(\frac{W}{2L(T)}\right)\left[\frac{\Delta}{2kT} - \frac{\lambda - 1}{2}\right] > 0$$

$$C(T) = (-\alpha R_{eh}(T) + \beta R_C(T) + \gamma R_S(T)) < 0. \tag{22}$$

It is noteworthy that a weak temperature dependence of the contact resistance (small values of β) and, especially, a negative temperature dependence of the contact resistance more readily give two inversion points.

If

$$A(T) < 0, \qquad B(T) < 0, \qquad C(T) < 0 \tag{23}$$

there is no inversion point.

A single inversion point takes place if $C(T) > 0$, i.e.,

$$C(T) = (-\alpha R_{eh}(T) + \beta R_C(T) + \gamma R_S(T)) > 0. \tag{24}$$

If the appropriate parameters of the structure are known, we can find from conditions (21)–(24) and equation (20) whether or not inversion points are present at any temperature and determine the current densities at which these inversion points occur.

Let us consider as an example a 4H-SiC rectifier diode of the 10 kV class with a 100 μm wide blocking base ($W = 100$ μm), room-temperature hole lifetime τ of 1.55 μs [15] and contact resistance at 300 K, R_C (300 K) $= 2.1 \times 10^{-3}$ Ω cm^2. The intrinsic concentration n_{i0} (300 K) $= 10^{-8}$ cm^{-3} [16], $\mu_n = 880$ cm^2 V^{-1} s^{-1}, $\mu_p = 120$ cm^2 V^{-1} s^{-1} [8], $Gp_0 = 5.8 \times 10^{19}$ V^{-1} cm^{-1} s^{-1} [3]. The substrate parameters are as follows: $W_n^+ = 300\,\mu$m, $N_D^+ = 5 \times 1019$ cm^{-3} and $\mu_n^+ = 30$ cm^2 V^{-1} s^{-1} [7]. The Auger recombination coefficients C_n^+ and C_p^+ were taken to be $C_n^+ = 5 \times 10^{-31}$ cm^6 s^{-1} and $C_p^+ = 2 \times 10^{-31}$ cm^6 s^{-1} [7].

When deriving (20), we neglected logarithmically weak dependence $V_{pn}(j)$. Hence, we need to preset the value of j at which $V_{pn}(T)$ is calculated in terms of the analytical model. Analysis shows that the best agreement between computer calculations and analytical estimates can be obtained for $V_{pn}(T)$ calculated at $j \sim 10^{-2}$ A cm^{-2}.

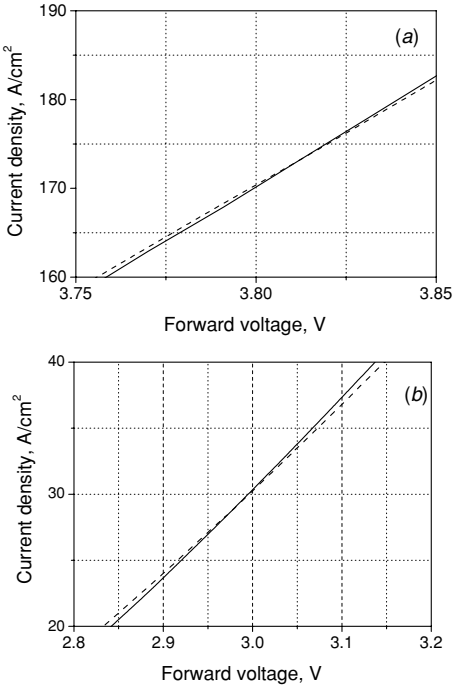

Figure 2. Current–voltage characteristics of a 4H-SiC diode (10 kV class), calculated using INVESTIGATION software. (*a*) Solid line: $T = 300$ K, dashed line: $T = 320$ K. (*b*) Solid line: $T = 600$ K, dashed line: $T = 620$ K, $W = 100$ μm, τ (300 K) $= 1.55$ μs, R_C (300 K) $= 2.1 \times 10^{-3}$ Ω cm^2, $\beta = 2.25$, n_{i0} (300 K) $= 10^{-8}$ cm^{-3}, $\mu_n = 880$ cm^2 V^{-1} s^{-1}, $\mu_p = 120$ cm^2 V^{-1} s^{-1}, $Gp_0 = 5.8 \times 10^{19}$ V^{-1} cm^{-1} s^{-1}. Emitter parameters: $W_n^+ = 300\,\mu$m, $N_D^+ = 5 \times 10^{19}$ cm^{-3}, $\mu_n^+ = 30$ cm^2 V^{-1} s^{-1}.

At the given values of the parameters, the coefficients in equation (20) at $T = 300$ K are as follows: $A(300) = -0.46$ V, $B(300) = 5.89 \times 10^{-3}$ V cm A$^{-1/2}$ and $C(300) = 3.11 \times 10^{-3}$ V cm^2 A^{-1}. At these values of the coefficients, equation (20) has just a single root corresponding to the current density $j_{in} \approx 172$ A cm^{-2}. Similar calculations for $T = 400$ K give $A(400) = -0.636$ V, $B(400) = 0.027$ V cm A$^{-1/2}$, $C(400) = 7.98 \times 10^{-3}$ V cm^2 A^{-1} and $j_{in} \approx 54.5$ A cm^{-2}. At $T = 600$ K, the parameters have the following values: $A(600) = -0.918$ V, $B(600) = 0.098$ V cm A$^{-1/2}$, $C(600) = 0.022$ V cm^2 A^{-1} and $j_{in} \approx 21.2$ A cm^{-2}.

The 'INVESTIGATION' ('ISSLEDOVANIE') software package [17] was used to calculate the inversion points for a p–i–n structure with the parameters listed above. This software package solves numerically a fundamental system of equations comprising two continuity equations (for electrons and holes) and a Poisson equation. The continuity equations are written in a form that takes into account all the main nonlinear phenomena in bipolar devices: electron–hole scattering, semiconductor bandgap narrowing and Auger recombination. The program also takes into account the decrease in the carrier lifetime and mobilities in the highly doped p$^+$ and n$^+$ layers. A detailed description of the software can be found in [18]. The Investigation software has already been used to analyse

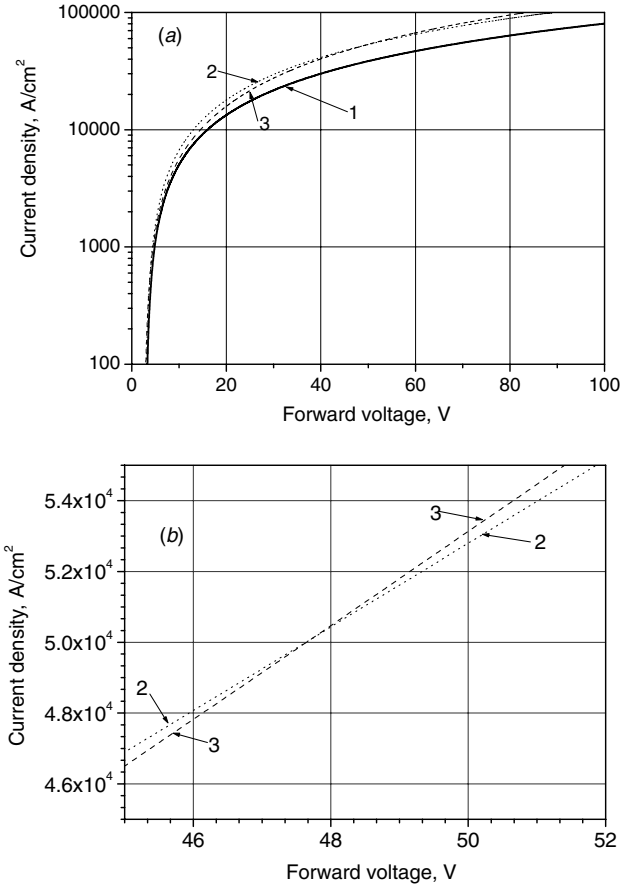

Figure 3. Calculated *I–V* characteristics of the diode at a small contact resistance R_C (300 K) = 2.1 × 10^{-6} Ω cm^2. All other parameters are the same as in figure 2. *T* (K): 1—300, 2—400, 3—600. (*a*) *I–V* characteristic in a wide range of current densities. (*b*) The same characteristic close to the second inversion point $j_{in\,2}$.

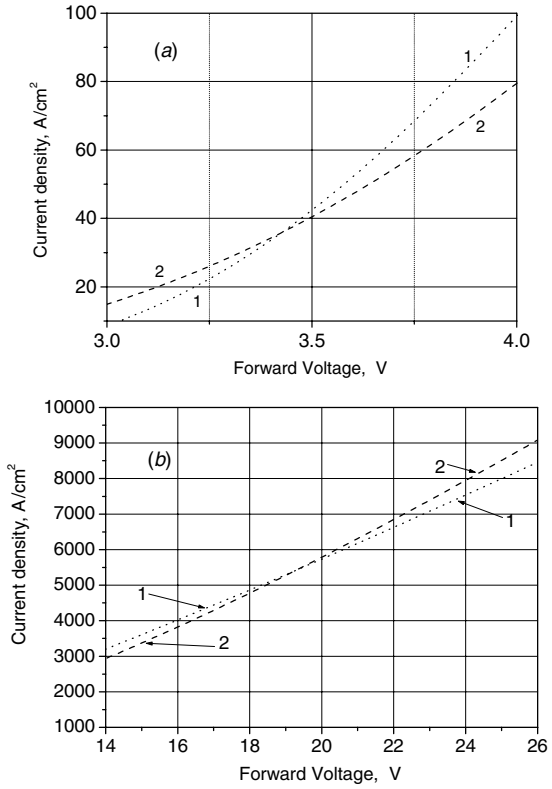

Figure 4. Calculated *I–V* characteristics of the diode with the same R_C (300 K) = 2.1 × 10^{-3} Ω cm^2 as that used for calculating the curves in figure 2, but with a negative temperature dependence of the forward bias ($\beta = -2.25$). *T* (K): 1—400, 2—600 (compare with figure 3). (*a*) *I–V* characteristics close to the first (low-current) inversion point ($j_{in} \approx 35$ A cm^{-2}), (*b*) *I–V* characteristics close to the second (high-current) inversion point ($j_{in\,2} \approx 5200$ A cm^{-2}).

steady-state and transient processes in high-voltage Si and SiC diodes and thyristors (see, for example, [15, 19, 20]).

Figure 2 shows the current–voltage characteristics of a 4H-SiC diode with the given parameters, calculated for temperatures of 300 and 320 K (figure 2(*a*)) and 600 and 620 K (figure 2(*b*)). In both cases, the results are shown for the current densities close to the inversion point j_{in}. As can be seen in figure 2, the current density corresponding to the room-temperature inversion point, $j_{in}(300) \approx 173$ A cm^{-2}; at $T = 600$ K, $j_{in}(600) \approx 28$ A cm^{-2}. We can conclude that the results of the computer simulation agree quite well with the analytical estimates made in the framework of the analytical theory.

It is important to note that the fact that j_{in} decreases as the temperature becomes higher improves the thermal stability of the device. Indeed, let us suppose that the current starts to increase spontaneously due to the negative differential conductivity of the device (figure 1(*b*)). As the current increases, the working temperature grows as well. Then, if the value of j_{in} also decreases with increasing temperature, the diode is turned off in the part of the *I–V* characteristic with a *positive* temperature coefficient of the isothermal voltage drop (figure 1(*a*)) and the rise in the current stops.

The analytical expressions (21)–(24) make it possible to analyse the effects of different parameters on the position of the inversion points. Let us consider, for example, the effect of the contact resistance R_C on the possible number of inversion points and their positions.

Figure 3(*a*) presents the calculated current–voltage characteristics of a diode with the set of parameters being the same as in figure 2, but with a contact resistance of R_C (300 K) = 2.1 × 10^{-6} Ω cm^2 [21]. It is easy to see that the inequality $C(T) < 0$ is valid for any temperature in the range 300–600 K. At $T = 300$ K, $\varphi\ (T) < 0$ (see equation (22)) and there is no inversion point in the *I–V* characteristic (curve 1 in figure 3(*a*)). At $T = 400$ K and $T = 600$ K, $\varphi\ (T) > 0$, and according to the analytical theory there are two inversion points in the *I–V* characteristics at these temperatures. Analytical estimates for the current density at the first inversion point give $j_{in} \approx 102$ A cm^{-2} and $j_{in} \approx 45$ A cm^{-2} for $T = 400$ and 600 K, respectively. As can be seen from figure 3, the computer calculations give $j_{in} \approx 110$ A cm^{-2} and $j_{in} \approx 51$ A cm^{-2} for $T = 400$ and 600 K, respectively in a very good agreement with the analytical estimates.

Figure 3(*b*) shows the same current–voltage characteristics as those in figure 3(*a*) ($T = 400$ and 600 K), but in the region close to the second inversion point $j_{in\,2}$. It can be seen that very high current densities $j_{in\,2} > 50$ kA cm^{-2} are characteristic of this case.

Figure 4 presents the calculated current–voltage characteristics of a diode with the same set of parameters

as in figure 2 and with the same R_C (300 K) = 2.1 × 10^{-3} Ω cm^2, but with a *negative* temperature coefficient $\beta = -2.25$. Figure 4(*a*) shows the *I–V* characteristics calculated for $T = 400$ and 600 K close to the first inversion point ($j_{in} \approx 35$ A cm^{-2}). Figure 4(*b*) demonstrates the same characteristics in the region of the second (high-current) inversion point $j_{in\,2}$. It is noteworthy that a rather moderate current density $j_{in\,2} \approx 5200$ A cm^{-2} corresponds to the second inversion point in the case under consideration. Such values of j are of practical interest in modes with current surges.

4. Conclusion

An analytical theory that makes it possible to determine the parameters of the inversion points in the current–voltage characteristics of high-voltage p–i–n rectifier structures has been suggested. It has been demonstrated that, depending on the set of the parameters, it is possible to observe zero, one or two inversion points in the current–voltage characteristics. The effects of the contact resistance and its temperature dependence on the parameters of the inversion points are analysed. The predictions of the theory are compared with the results of adequate numerical experiments for a high-voltage (10 kV class) 4H-SiC p^+–i–n diode. The results of the computer experiments coincide well with the predictions of the analytical theory.

Acknowledgments

This work was supported by Cree Inc. At the All-Russia Electrotechnical Institute and at the Ioffe Institute this work was supported by the Russian Foundation for Basic Research (grants 05-02-16541, 05-02-17768, 05-08-18235).

References

[1] Sze S M 1981 *Physics of Semiconductor Devices* (New York: Wiley)
[2] Shur M S 1990 *Physics of Semiconductor Devices* (Englewood Cliffs, NJ: Prentice-Hall)
[3] Mnatsakanov T T, Levinshtein M E, Ivanov P A, Palmour J W, Tandoev A G and Yurkov S N 2003 *J. Appl. Phys.* **93** 1095
[4] Sugawara Y, Takayama D, Asano K, Singh R, Palmour J and Hayashi T 2001 *Proc. of 2001 Int. Symp. on Power Semiconductor Devices & ICs (Osaka, Japan)* pp 27–30
[5] Davies L V 1962 *Nature* **194** 702
[6] Herlet A 1968 *Solid-State Electron.* **11** 717
[7] Mnatsakanov T T, Shuman V B, Pomortseva L I, Schroder S and Schlogl A 2000 *Solid-State Electron.* **44** 383
[8] Levinshtein M E, Rumyantsev S L and Shur M S (ed) 1996 *Handbook Series of Semiconductor Parameters, vol 1: Elementary Semiconductors and A3B5 Compounds Si, Ge C, GaAs, GaP, GaSb InAs, InP, InSb* (Singapore: World Scientific)
[9] Levinshtein M E, Rumyantsev S L and Shur M S (ed) 2001 *Properties of Advanced Semiconductor Materials: GaN AlN, InN, BN, SiC, SiGe* (New York: Wiley)
[10] Huldt L, Nilsson N G and Svantesson K G 1979 *Appl. Phys. Lett.* **35** 776
[11] Varshni Y P 1967 *Physica* **34** 149
[12] Ivanov P A, Levinshtein M E, Irvin K G, Kordina O, Palmour J W, Rumyantsev S L and Singh R 1999 *Electron. Lett.* **35** 1382
[13] Agarwal A K, Ivanov P A, Levinshtein M E, Palmour J W, Rumyantsev S L and Ryu Sei-Hyung 2001 *Semicond. Sci. Technol.* **16** 260
[14] Mnatsakanov T T, Pomortseva L I and Yurkov S N 2001 *Semiconductors* **35** 394
[15] Levinshtein M E, Mnatsakanov T T, Ivanov P A, Singh R, Palmour J W and Yurkov S N 2004 *Solid-State Electron.* **48** 807
[16] Ivanov P A, Levinshtein M E, Palmour J W, Rumyantsev S L and Singh R 2000 *Semicond. Sci. Technol.* **15** 908
[17] Mnatsakanov T T, Rostovtsev I L and Philatov N I 1987 *Solid-State Electron.* **30** 579
[18] Levinshtein M E, Mnatsakanov T T, Ivanov P A, Palmour J W, Rumyantsev S L, Singh R and Yurkov S N 2001 *IEEE Trans. Electron Devices* **48** 1703
[19] Levinshtein M E, Mnatsakanov T T, Ivanov P A, Palmour J W, Rumyantsev S L, Singh R and Yurkov S N 2000 *Electron. Lett.* **36** 1241
[20] Mnatsakanov T T, Levinshtein M E, Ivanov P A, Palmour J W, Das M and Agarwal A K 2005 *Semicond. Sci. Technol.* **20** 62
[21] Chang S C, Wang S J, Uang K M and Liou B W 2005 *Solid-State Electron.* **49** 1937